Fracture Toughness of Adhesive Joints. II. Temperature and Rate Dependencies of Mode I Fracture Toughness and Adhesive Tensile Strength

WON WOO LIM* and HIROSHI MIZUMACHI

Division of Chemistry of Polymeric Materials, Department of Forest Products Science, Faculty of Agriculture, The University of Tokyo, Bunkyo-ku, Tokyo 113, Japan

SYNOPSIS

It has been known that adhesive strength shows temperature and rate dependencies reflecting visoelastic properties of an adhesive. Similarly, a critical strain energy release rate is expected to show temperature and time dependencies because deformation and fracture of the adhesive occurs at the time of measurement of the critical strain energy release rate, which is a kind of fracture mechanical parameter for adhesive joints. The term "critical strain energy release rate" has usually been called "fracture toughness." In this study, the critical strain energy release rate (G_{IC}) of the opening mode was called mode I fracture toughness. G_{IC} was measured over a wide range of temperatures and rates, and then a master curve was obtained by applying the temperature–rate superposition principle to the obtained data. Also, on the relation between G_{IC} and adhesive tensile strength is discussed.

INTRODUCTION

A polymer used as an adhesive is a viscoelastic material, and its mechanical properties are dependent on experimental conditions, especially temperature and time scale (strain rate, frequency). A series of time-scale dependencies on the linear viscoelastic properties of the polymer were measured at various temperatures, and a master curve was then obtained by applying the time–temperature superposition principle to the obtained data. We can obtain viscoelastic functions over a wide range of time scales from the master curve. It has been known that a shift factor, a_T, used to obtain the master curve is expressed by the Williams–Laudel–Ferry (WLF) or Arrhenius equation.[1-4]

T. L. Smith[5] studied the rupture of various elastomers systematically, and showed that the temperature–rate superposition principle apparently could be applied to the mechanical behaviors of large deformation and failure, and that the master curves for the ultimate stress and strain at rupture could be obtained. In addition, he also showed that the shift factor followed the WLF equation.

In addition to the fact that the ultimate stress and strain at rupture depend on the inherent structure and physical properties of a material itself, it is well known that microvoids inside the material and other flaws can significantly alter the fracture behavior. Recently, the fracture mechanical approach has frequently been tried with emphasis on the latter. Bitner et al.[6] showed that the fracture energy of rubber-modified epoxy, which is a structural adhesive, could be described as a function of both temperature and time-to-failure, and they pointed out that the value significantly changed around the glass transition temperature, T_g. Huang and Kinloch[7] also expressed the fracture energy as a function of the temperature and rate of testing where compact-tension specimens of similar rubber-modified epoxy resin were used, and clarified that the master curve could be obtained.

The performance of adhesive joints is usually evaluated in terms of a series of adhesive strength tests. The fracture behavior in the adhesive test is very complicated because the cohesive fracture of adhesive, interfacial fracture, cohesive fracture of

* To whom correspondence should be addressed.

Journal of Applied Polymer Science, Vol. 57, 55–61 (1995)
 CCC 0021-8995/95/010055-07

Table I Description of Adhesives

	KU661	KU662
Component	Polyester(polyol)	Polyisocyanates
Specific gravity	1.13	1.23
Viscosity (cps/25°C)	6000–15000	100–250
Mixing ratio, parts by weight	100	100
Work life at 20°C	30–40 min (mixture)	

the adherend itself, or fracture of mixed modes can occur. Nevertheless, it is experimentally confirmed that the adhesive strength measured by the standardized test methods shows systematic temperature and rate dependencies in most cases, and the application of the temperature and rate superposition principle to this complex behavior was attempted by many researchers. The researchers found that the shift factor changed according to the change of fracture modes.[8-13]

On the other hand, the data on rheological properties of the critical strain energy release rate for the adhesive joints has not been sufficiently studied. We clarified the fundamental conditions to empirically estimate the critical strain energy release rates (G_{IC}, G_{IIC}, G_{IIIC}) in the opening mode, plane-shear mode, and tearing-shear mode.[14] The term "critical strain energy release rate" is usually called "fracture toughness." In this study, critical strain energy release rate (G_{IC}) in the opening mode is called "mode I fracture toughness." G_{IC} for the adhesive joints bonded with polyurethane adhesive was measured over a wide temperature range and rates. Thus, we examined whether or not the temperature–rate superposition principle can be applied to the obtained data. Further, we considered the relation between G_{IC} and the adhesive tensile strength, both of which have similar deformation modes.

EXPERIMENTAL

Materials

Polyurethane adhesives, KU661 and KU662 (Konishi Company), were used in this work. This adhesives consist of polyester(polyol) (KU661) and polyisocyanates (KU662). The characteristics of the adhesives are summarized in Table I.

Kaba, the Japanese birch, (Betula maximowiczana Regel), finished with surface planer (Hitachi Co.) was used as an adherend, the physical properties of which are shown in Table II.

Measurement of Dynamic Mechanical Properties

The cured film was prepared by casting the mixture of KU661 and KU662 on a Teflon sheet and curing the mixture at room temperature and 65% relative humidity (RH) for 5 days. Dynamic mechanical properties of the film were measured by means of a Rheovibron DDV-II (Toyo Baldwin Co., Ltd.) at 110 Hz with an average heating rate of 1°C/min.

Measurement of G_{IC} for Adhesive Joints

Wood specimens for fracture mechanical tests were prepared with grain angle of 5° as shown in Figure 1, which is the angle necessary to prevent wood failure along the grain prior to fracture. Precracked length was 8 cm, referring to the previous work.[14] The amount of adhesive employed was 250–300 g/cm^2, and the specimen was assembled as shown in Figure 1.

The specimen was pressed under 10 kg/cm^2 and kept at 20°C, 65% RH for 4 days for curing. The fracture mechanical test was carried out with crosshead speeds of 0.5, 5.0, 50.0, and 500.0 mm/min over a range of −60–80°C by means of a Tensilon tester (Orientec Co.). G_{IC}, was determined by the compliance method according to the following equation[15,16]:

Table II Characteristics of Adherend

Adherend	Specific Gravity: Air Condition	Specific Gravity: Dry Condition	Moisture Content (%)	Young's Modulus, E (10^5 kgf/cm^2)
Kaba	0.88	0.78	14.9	1.16

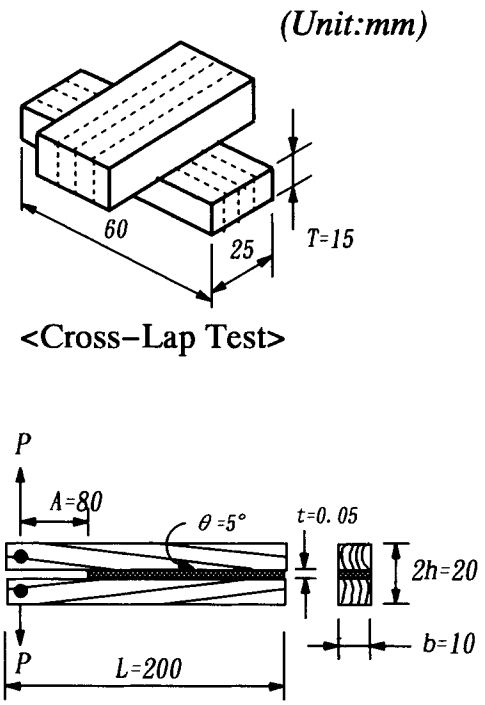

Figure 1 Dimensions of specimens.

$$G_{IC} = \frac{4P_c^2}{b^2E}\left[\frac{3A^2}{h^3} + \frac{1}{h}\right] \quad (1)$$

where P_C and E are failure load and Young's modulus of the adherend, respectively, and the other parameters are shown in Figure 1.

Measurement of Adhesive Tensile Strength

The specimen for the cross-lap test was prepared as shown in Figure 1. The adhesion conditions, such as spread amount of adhesive and bonding pressure, were the same as that of the fracture mechanical test described. The measurement of adhesive tensile strength was carried out with crosshead speeds of 0.5, 5.0, and 50.0 mm/min over a range of −60°–80°C using the Tensilon tester.

RESULTS AND DISCUSSION

Temperature and Rate Dependencies of G_{IC}

Figure 2 shows the dynamic mechanical properties for an adhesive used in this work. A primary transition and a secondary transition appeared at 46 and −60°C, respectively. It is expected that the viscoelastic properties of the adhesive strongly affect the fracture mechanical properties of adhesive joints.

Figure 3 shows the temperature dependence of G_{IC} in the opening mode for the adhesive joints. G_{IC} is maximized at a glass transition temperature of the adhesive. This result suggests that the fracture behavior reflects an energy dissipation mechanism based on the micro-Brownian motion of the main chain of the adhesive. G_{IC} increased with decreasing temperature. We do not have enough data to tell whether the existence of a secondary transition affected this temperature dependence of G_{IC} or not. The curve of G_{IC} shifted to a higher temperature region with increasing crosshead speeds.

Equation (2) holds for G_{IC} of the adhesive joints bonded with viscoelastic adhesive.

$$G_{IC}(\nu) = \left(\frac{T}{T_0}\right)^2 G_{IC0}(\nu a_T) \quad (2)$$

where ν is rate, a_T shift factor, G_{IC} and G_{IC0} mode I fracture toughness at temperature T and T_0, respectively.

Applying the temperature–rate superposition principle to these data, we obtained a master curve, which is shown in Figure 4. We can get information on G_{IC} over a very wide range of rates from this master curve. The peak of G_{IC} centered at around $V \cdot a_T = 1.0 \times 10^{-3}$ mm/min was considered to correspond to a primary transition of the adhesive polymer. It is not obvious whether G_{IC} reaches a maximum at higher rates ($V \cdot a_T > 1.0 \times 10^6$ mm/min) or not.

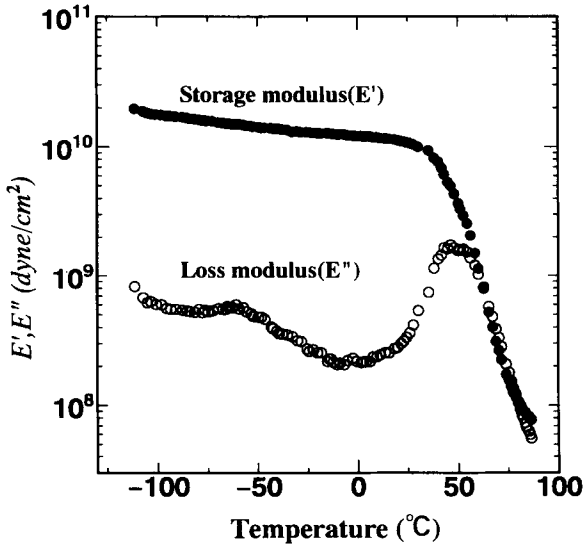

Figure 2 Dynamic mechanical properties of adhesives KU661 and KU662.

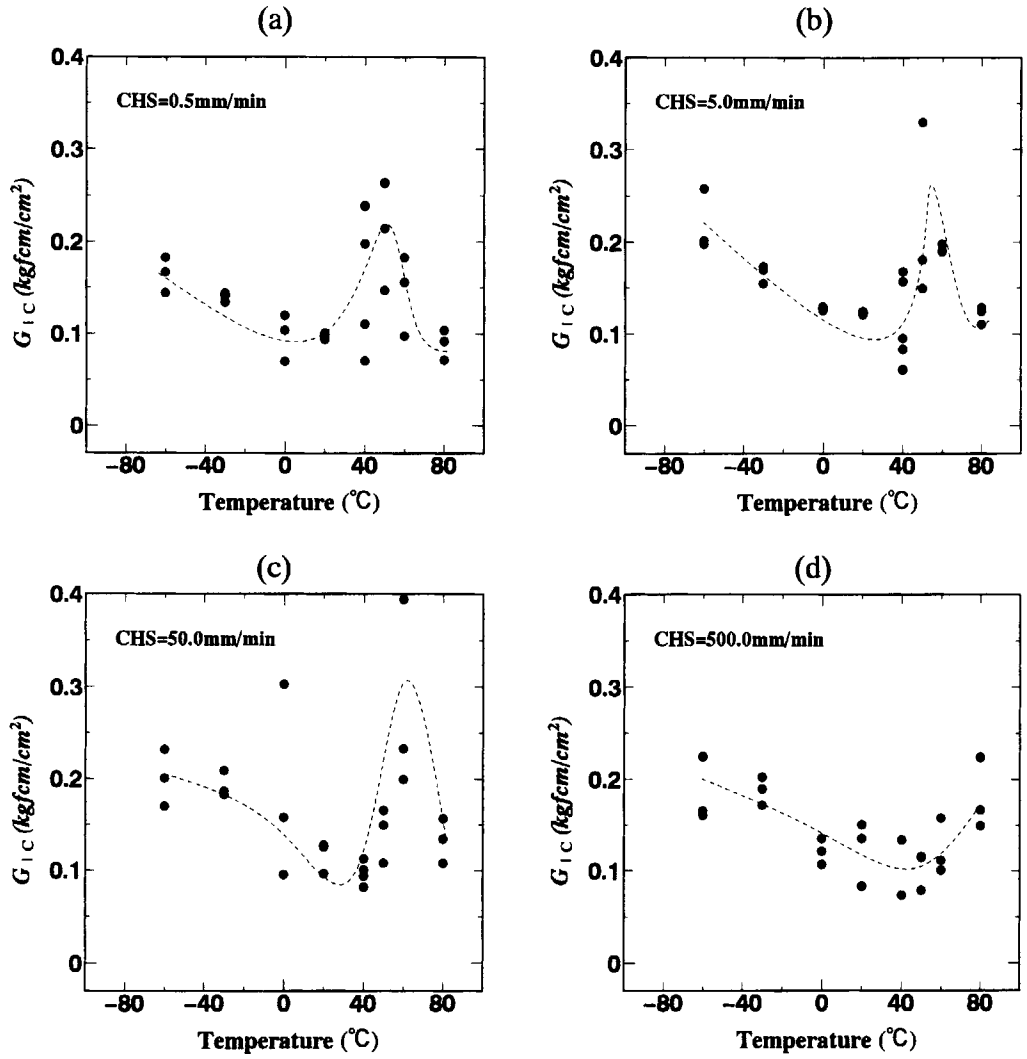

Figure 3 Temperature dependence of G_{IC} at various crosshead speeds: (a) 0.5, (b) 5.0, (c) 50.0, and (d) 500.0 mm/min.

The failure modes in fracture mechanical tests were interfacial and cohesive in a lower temperature region and in a higher temperature region, respectively. Both interfacial fractures and cohesive fractures occurred at the same time in the transition region. The experimental shift factors, a_T, which were used to obtain the master curve, and the Arrhenius equation are plotted in Figure 5. The experimental shift factors fitted the Arrhenius equation, and two straight lines were clearly observed. The apparent activation energy was 51 and 14 kcal/mol for the higher and the lower temperature regions, respectively. The different apparent activation energy corresponds to different fracture modes. Similar features were also found when conducting a peeling test, which means that both the fracture test in the opening mode and the peel test have similar deformation and fracture processes.[17]

Temperature and Rate Dependencies of Adhesive Tensile Strength

Figure 6 shows the temperature dependence of the adhesive tensile strength for the cross-lap test, where the wood specimens were bonded with the same adhesive. In a lower temperature region, it was 20–40 kgf/cm^2. The value increased with increasing temperature. Subsequently the value reached a maximum of adhesive tensile strength at a temperature and then tended to decline. Wood failure or cohesive fracture of the adherend was greater at a temperature region lower than that corresponding to the

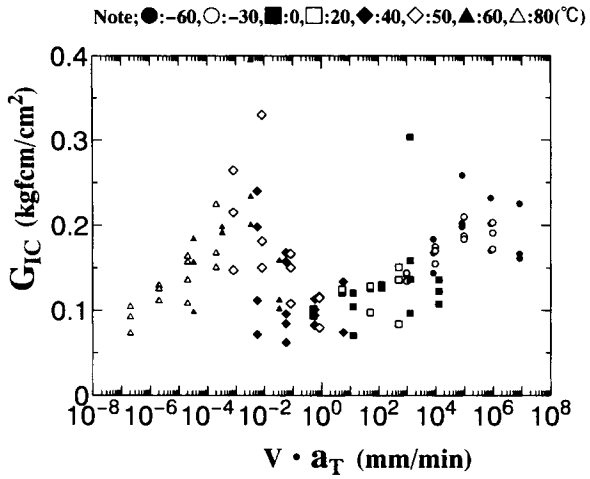

Figure 4 Master curve of G_{IC} reduced to 20°C.

maximum value. This means that when the adhesive is stiff, failure along the grain of the wood tends to occur. At higher temperatures, the adhesive tensile strength decreased as the storage modulus (E') of the adhesive decreased because cohesive strength of the adhesive decreased at higher temperatures. In other words, resistance of the adhesive layer against external forces decreases and cohesive fracture of the adhesive layer primarily occurs. The curve of the adhesive tensile strength shifts to a higher temperature region with increasing crosshead speed. Figure 7 shows the master curve obtained by applying the temperature–rate superposition principle to the data according to the same shift factor shown in Figure 6. The adhesive tensile strength showed a

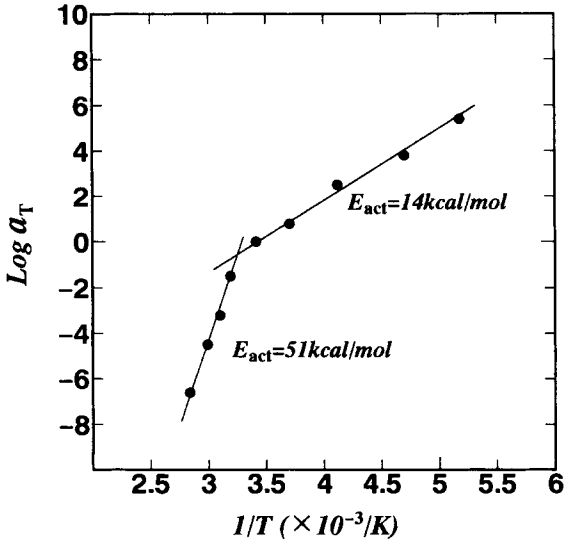

Figure 5 Arrhenius plot of shift factor, log a_T (E_{act} is an apparent activation energy).

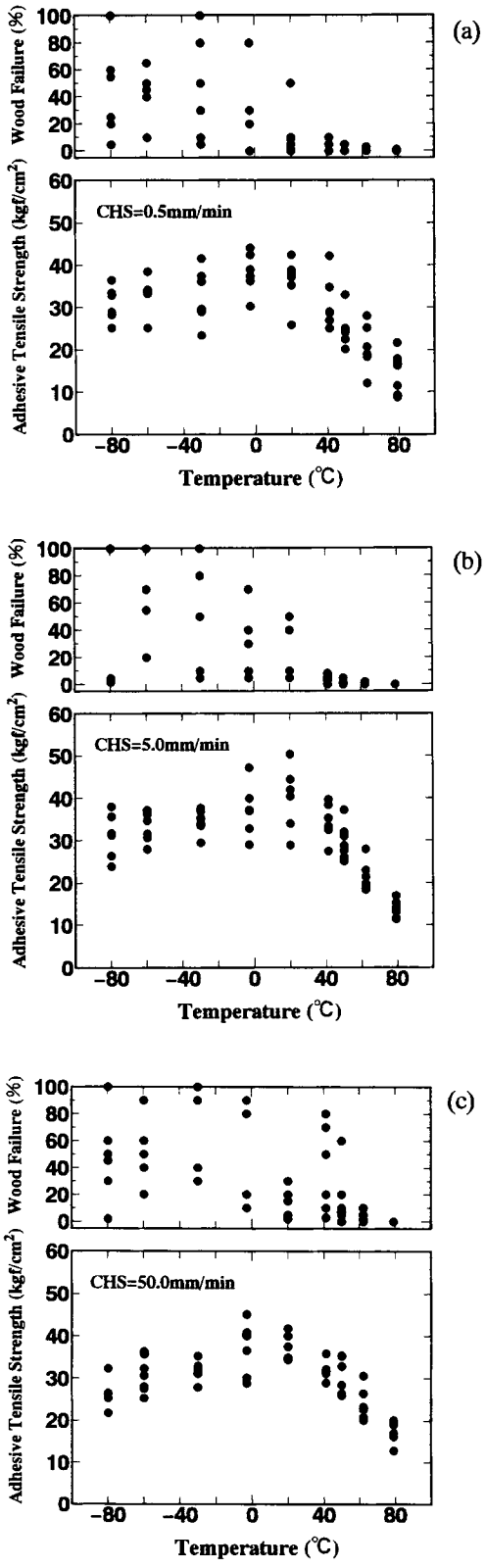

Figure 6 Temperature dependence of adhesive tensile strength at various crosshead speeds: (a) 0.5, (b) 5.0, and (c) 50.0 mm/min.

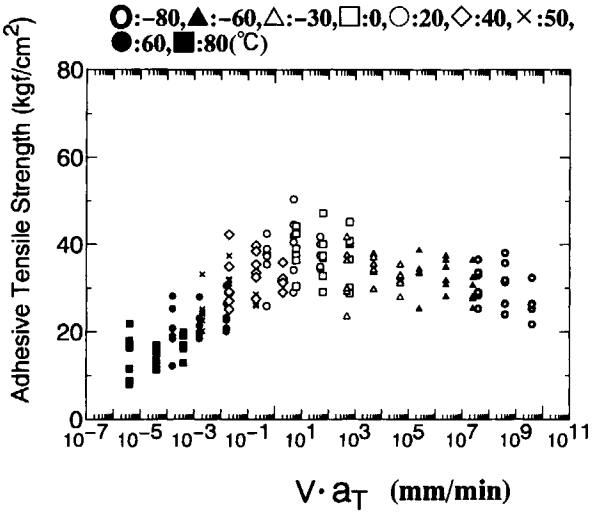

Figure 7 Master curve of adhesive tensile strength reduced to 20°C.

clear peak at around $V \cdot a_T$ = 10 mm/min, and was nearly constant at higher rates.

Relationship Between G_{IC} and an Adhesive Tensile Strength

The results of the adhesive tensile test and the fracture mechanical test for a specimen bonded with polyurethane adhesive showed that G_{IC} and adhesive tensile strength were strongly dependent on temperature and time scale. These two tests involve similar deformation processes, but their physical meanings are somewhat different from each other.

Figure 8 shows the relationship between G_{IC} and adhesive tensile strength. First, a positive correlation between the square root of G_{IC} and the adhesive tensile strength was found with a lower rate or a higher temperature region. In this region, G_{IC} and adhesive tensile strength were strongly dependent on the modulus of the adhesive, and both decreased with decreasing E' in the region where cohesive fracture of the adhesive mostly occurred. In a stress–strain curve, stress increased with an increase in strain in the first step, and after yielding, nonlinear behavior was found between stress and strain. When a crack propagated at this step, brittle and ductile fractures occurred simultaneously.

However, no correlation could be found between the square root of G_{IC} and the adhesive tensile strength with a higher rate or a lower temperature region. In this region, the deformation of the adhesive layer was relatively small because the adhesive was in a glassy state. Interfacial fracture occurred in the fracture mechanical test and cohesive fracture of the adherend occurred in the adhesion test. Because the surface structure of the wood adherend is complicated, stress concentration caused by external forces may be different from specimen to specimen, and this may be the reason why we find scatters of points in Figure 8. The stress–strain behavior for the fracture mechanical test was semi-elastic and a little plastic deformation was observed after yielding. Brittle fracture occurred because the crack propagated at this step.

From these results, we came to believe that there is a positive correlation between the square root of G_{IC} and the adhesive tensile strength in the lower rate or the higher temperature region because similar deformation proceeded in both tests and because cohesive fracture of the adhesive layer occurred. However, in the higher rates or lower temperature region, any distinct correlation between the square root of G_{IC} and the adhesive tensile strength could not be found because the location of fracture in both tests were different from each other.

CONCLUSION

G_{IC} and adhesive tensile strength of woods bonded with polyurethane adhesives varied as a function of both temperature and rate dependencies, reflecting the viscoelastic properties of the adhesive. G_{IC} and adhesive tensile strength achieved high value or maximums at around the T_g or at a rate correspond-

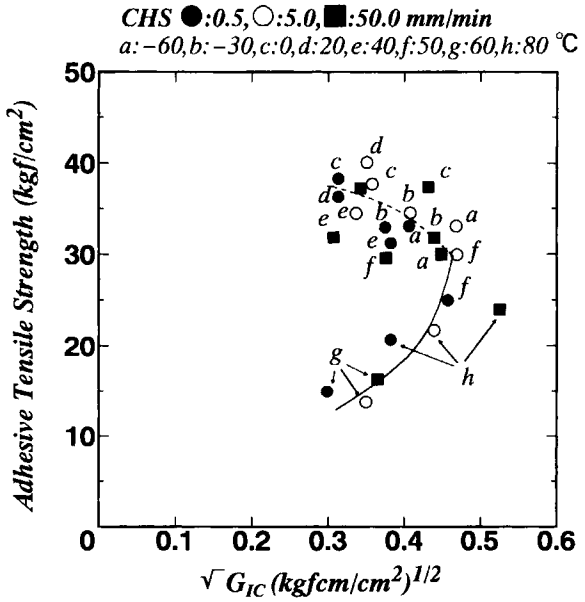

Figure 8 Relationship between G_{IC} and adhesive tensile strength. CHS, crosshead speed.

ing to the T_g of the adhesive. Applying the temperature–rate superposition principle to the experimental data, we obtained the master curves of both G_{IC} and adhesive tensile strength. Two straight lines were observed in the Arrhenius plot of the shift factor log a_T. This indicates that different fracture mechanisms existed.

A positive correlation was observed between the square root of G_{IC} and adhesive tensile strength at a lower rate or in a higher temperature region. However, clear correlation between the square root of G_{IC} and adhesive tensile strength could not be found at a higher rate or in a lower temperature region. Further, the correlation between these two values was strongly related to the viscoelastic properties of the adhesive and the fracture modes of the joints.

The accumulation of systematic data is required to clarify the correlation between G_{IC} and adhesive tensile strength for a variety of conventional adhesives.

REFERENCES

1. M. L. Williams, R. F. Landel, and J. D. Ferry, *J. Am. Chem. Soc.*, **77,** 3701 (1955).
2. F. Bueche, *Physical Properties of Polymer,* Wiley, New York, 1970.
3. J. D. Ferry, *Viscoelastic Properties of Polymers,* Wiley, New York, 1970, Chap. 11.
4. A. V. Tobolsky, *Properties and Structure of Polymers,* Wiley, New York, 1960, Chap. 4.
5. T. L. Smith, *J. Polym. Sci.*, **32,** 99–113 (1958).
6. J. L. Bitner, J. L. Rushford, W. S. Rose, D. L. Hunston, and C. K. Riew, *J. Adhesives,* **13,** 3–28 (1981).
7. Y. Huang and A. J. Kinloch, *J. Adhesives,* **41,** 5–22 (1993).
8. K. Motohashi, B. Tomita, H. Mizumachi, and H. Sakaguchi, *Wood Fiber Sci.*, **16,** 72–85 (1984).
9. T. Kobayashi, Y. Hatano, and H. Mizumachi, *Mokuzai Gakkaishi,* **37,** 324–330 (1991).
10. A. N. Gent and R. P. Petrich, *Proc. Roy. Soc. A.*, **310,** 433–448 (1969).
11. A. N. Gent, *J. Polym. Sci. A-2,* **9,** 283–294 (1971).
12. A. Ahagon and A. N. Gent, *J. Polym. Sci. Polym. Phys.*, **13,** 1285–1300 (1975).
13. T. Hata, M. Gamou, K. Kojima, and T. Nakamura, *Kobunshikagaku,* **22,** 160 (1965).
14. W. W. Lim, Y. Hatano, and H. Mizumachi, *J. Appl. Polym. Sci.*, **52,** 967–973 (1994).
15. S. Mostovoy and E. J. Ripling, *J. Appl. Polym. Sci.*, **15,** 641–659 (1971).
16. S. Mostovoy and E. J. Ripling, *J. Appl. Polym. Sci.*, **15,** 661–673 (1971).
17. Y. Hatano and H. Mizumachi, *Mokuzai Gakkaishi,* **35,** 243–250 (1989).

Received October 25, 1994
Accepted December 20, 1994